# Multi-objective optimization of thermoplastic CF/PEKK drilling through a hybrid method: an approach towards sustainable manufacturing

## Published in:
Composites Part A: Applied Science and Manufacturing

## Document Version:
Publisher's PDF, also known as Version of record

## Queen's University Belfast - Research Portal:
Link to publication record in Queen's University Belfast Research Portal

# Multi-objective optimization of thermoplastic CF/PEKK drilling through a hybrid method: An approach towards sustainable manufacturing

Jia Ge [a], Wenchang Zhang [b], Ming Luo [b], Giuseppe Catalanotti [a,c], Brian G. Falzon [a,d,e], Colm Higgins [f], Dinghua Zhang [b], Yan Jin [a], Dan Sun [a,*]

[a] School of Mechanical and Aerospace Engineering, Queen's University Belfast, Belfast BT9 5AH, UK
[b] School of Mechanical Engineering, Northwestern Polytechnical University, Xi'an, PR China
[c] Escola de Ciências e Tecnologia, Universidade de Évora, 7000-671 Évora, Portugal
[d] RMIT Space Industry Hub, STEM College, RMIT University, Melbourne, Victoria 3000, Australia
[e] Aerospace Engineering and Aviation, School of Engineering, RMIT University, Melbourne 3000, Australia
[f] Northern Ireland Technology Centre (NITC), Queen's University Belfast, Belfast BT9 5AH, UK

## ARTICLE INFO

## ABSTRACT

Carbon-fibre-reinforced-polyetherketonketone (CF/PEKK) has attracted increasing interest in the aviation industry due to its self-healing properties and ease of recycle and repair. However, the machining performance of CF/PEKK is not well understood and there is a lack of optimization study for minimizing its hole damage and improving the production efficiency. Here, we report the first multi-objective optimization study for CF/PEKK drilling. A hybrid optimization algorithm integrating Non-dominated Sorting Genetic Algorithm-II (NSGA-II) and Techniques for Order of Preference by Similarity to Ideal Solution (TOPSIS) is deployed to obtain the Pareto solutions and rank the multiple solutions based on closeness to ideal solutions. To highlight the impact of different matrix properties on the optimization outcome, comparative study with conventional thermoset carbon fibre reinforced epoxy composite (CF/epoxy) is carried out for the first time. Experimental validation shows the proposed method can achieve 91.5–95.7% prediction accuracy and the Pareto solutions effectively controlled the delamination and thermal damage within permissible tolerance. The vastly different optimal drilling parameters identified for CF/PEKK as compared to CF/epoxy is attributed to the thermoplastic nature of CF/PEKK and the unique thermal/mechanical interaction characteristics displayed during the machining process.

## 1. Introduction

In order to reduce the carbon footprint for the benefit of the global economy, environment and social well-being, utilization of more sustainable materials and enhancing materials manufacturing efficiency become ever important for the modern aerospace industry [1,2]. In recent years, carbon fibre reinforced thermoplastics (CFRTPs), particularly carbon fibre reinforced polyetherketoneketone (CF/PEKK), have been increasingly used in new generation light-weight aircraft structures [2–4]. Compared to conventional thermoset carbon fibre reinforced plastics (e.g. CF/epoxy) [5], CF/PEKK offers excellent mechanical performance and better interlaminar/intralaminar fracture toughness [6,7]. The thermoplastic nature of the PEKK matrix also opens a new avenue towards aircraft self-repair [8] and recycling [9], making CF/PEKK a promising candidate for more sustainable aircraft structures.

Although certain CFRTP parts can be manufactured into net shape or assembled through welding [10], mechanical fastening through riveting holes still remains an imperative joining process [11,12], particularly for load bearing components [13,14] and joints consisting of dissimilar materials (e.g. metal/CFRTP). Drilling, being the most efficient hole making technique, is still widely used in the aircraft assembly process [15]. Similar to drilling of CF/epoxy, CFRTP suffers from hole damage (such as delamination [4], burrs [16], hole circularity surface [17], microstructural damages [18], etc) when improper/sub-optimal drilling conditions are deployed. These damages will inevitably affect the hole quality, lower the component's mechanical performance and subsequently compromise the aircraft reliability. Unsatisfactory hole quality (e.g. delamination damage) can account up to 60% part rejection in aircraft assembly [19]. To date, the drilling performance of CFRTP remains a significant but understudied subject in the literature [20,21],

and optimizing drilling parameters for new generation CFRTP plays a crucial role in low-damage, high-efficiency and cost effective future aircraft sustainable manufacturing.

Most of composite drilling optimization studies in the literature have been focused on conventional CF/epoxy [22]. Since the optimization usually involves multiple objectives (e.g. a range of hole quality metrics and production efficiency, etc), some early researchers dealt with such multi-objective optimization problem using the weighted sum method [23]. Specifically, a set of weighting factors were deployed to convert a multi-objective problem into a traditional single-objective solution. For instance, Feito et al. [24] designed a full factorial experiment for multi-objective optimization of CF/epoxy drilling. Analysis of variance (ANOVA) was utilized to reveal the effect of feed rate, cutting speed and tool geometry on drilling thrust force, torque and hole delamination. The relationship between input and output variables was established by means of response surface methodology (RSM). The multi-objective problem was converted to a single-objective problem through assigning weighting factors according to the relative importance of each objective. Results showed that low feed rate (0.05 mm/rev) was preferable under all conditions. However, the optimal cutting speed can be greatly affected by the value of weighting factors assigned to each objective. In another study by Feito et al. [25], optimization of CF/epoxy woven composite drilling was conducted under different tool wear conditions. Optimization results suggest the optimal cutting speed should be increased from ~25 m/min to ~100 m/min with growing tool wear. Soepangkat et al. [26] developed an integrated back propagation neural network-particle swarm optimization (BPNN-PSO) method for CF/epoxy drilling. Experiments validated the satisfactory prediction performance of BPNN-PSO with error less than 5% and the micro-structural/delamination damages were effectively minimized under the optimal feed rate (79 mm/min) and spindle speed (2933 rpm). Abhishek et al. [27] applied a fuzzy embedded harmony search (HS) algorithm for CF/epoxy drilling optimization. When compared with genetic algorithm (GA), HS showed better efficiency in searching optimal solutions with less computational cost. For the above-mentioned studies, by incorporating multi-objective functions into a single scalar fitness function, a single optimal solution which minimizes/maximizes the overall performance can be achieved. However, such optimization results may be biased as they depend highly on the assigned weight factors, which are usually based on expert knowledge or personal preferences [28]. Additionally, the optimization study on machining of CFRTP, particularly CF/PEKK drilling, is very limited.

In recent years, several researchers deployed 'Pareto method' in multi-objective optimization of composite drilling. A set of optimal solutions (Pareto front) rather than a single optimal solution were obtained, hence an insight into trade-off between multiple objectives can be established. Sardinas et al. [29] was the first to utilize such method, where GA algorithm was used to optimize two conflicting objectives in CF/epoxy drilling (material removal rate and delamination damage). Later, Wang et al. [30] developed a method integrating BPNN, Non-dominated Sorting Genetic Algorithm-II (NSGA-II) and fuzzy c-means clustering to optimize the CF/epoxy drilling thrust force, delamination damage and production efficiency. Nine representative solutions were selected from the Pareto front for experiment validation and the model showed average errors of 3.21% and 1.11% for thrust force and delamination prediction, respectively. Despite these promising results, the large number of solutions present in the Pareto front remains a challenge for determining the most appropriate/satisfactory solution for experimental verification and practical implementation.

Development and utilization of multi-criteria decision making (MCDM) algorithms could effectively address the above mentioned challenge by selecting the preferable solution from the set of Pareto optimal solutions [31]. Techniques for Order of Preference by Similarity to Ideal Solution (TOPSIS) is a highly effective MCDM method [32]. This method evaluates and finds the optimal solution based on the criteria that preference is given to those solutions with the closest Euclidean distance to the ideal solution and largest distance to the negative-ideal solution. TOPSIS is highly computationally efficient and has good comprehensibility in evaluating various alternatives and achieving rational trade-off between criteria [33]. Jadhav et al. [34] proposed an optimization method combining artificial neural network (ANN), GA and TOPSIS for improving the performance of Nimonic C-263 superalloy cryogenic assisted turning. This hybrid approach achieved a prediction accuracy over 93 % and has effectively improved the closeness factor. Li et al. [33] carried out multi-objective optimization of CF/epoxy trimming combining neural network and TOPSIS to minimize surface roughness, tool temperature and tool flank wear. The optimal solutions have effectively improved the closeness coefficient and the prediction accuracy was verified by experiment. Liu et al. [35] deployed a hybrid approach combining GA-BP neural network, NSGA-II and TOPSIS for multi-objective optimization of high speed CF/PEEK milling. The prediction accuracy was over 90% and the optimal milling parameters selected from the Pareto front have effectively eliminated the surface defects such as fibre fracture and matrix smearing. Despite the effectiveness of TOPSIS, hybrid methods integrating multi-objective optimization and TOPSIS is still in its infancy and such hybrid optimization has never been attempted under the context of composite drilling.

Here we report the first multi-objective optimization study for CF/PEKK drilling with the aim of minimizing hole damage (thrust force and delamination damage) and maximizing production efficiency (material removal rate). It is the first time a multi-objective optimization algorithm (NSGA-II) was integrated with a MCDM algorithm (TOPSIS) to determine the top-ranking composite drilling solution within the Pareto front. Additionally, given CF/PEKK's distinctly different thermal/mechanical properties from conventional CF/epoxy, we hypothesize that the optimization results of the two materials may not be directly transferable. Therefore, the optimization of thermoset CF/epoxy drilling is also conducted to verify our hypothesis and establish new insights into the impact of different matrix properties / drilling performance on the optimization outcome. The optimization results for both composites were then verified by experiments to demonstrate the validity of the proposed method.

## 2. Experiment setup

### 2.1. Materials and drilling experiment setup

CF/PEKK laminates were manufactured from unidirectional (UD) prepregs using heated press following supplier's specifications [36]. CF/epoxy laminates (manufactured with T700S/2592 UD prepregs) were provided by Shenzhen Jinjiuyi Electronic Technology Co., Ltd, China. Both composites were 3 mm in thickness and consist of 22 plies to form a cross-ply stacking sequence. The composite laminates were cut by water jet into 120 mm square workpiece. Both composites contain 60 vol% carbon fibre of the same grade with modulus of elasticity and tensile strength of 240 and 4.8 GPa, respectively.

The drilling experiment was carried out under dry condition following established setup [4] using 3 axis Deckle FP3A CNC machine (Heidenhain TNC 355 system, see Fig. 1 (a)) and Aitefasi drill bits (Aitefasi Tools Co., Ltd, China, TiAlN coated solid carbide drill, see Fig. 1 (b)). A full factorial experiment was performed using four levels of spindle speeds ($S$) and five levels of feed rates ($F_f$), see Table 1. The drilling parameters are selected in accordance with the literature [4,18] and tool suppliers' recommendation. Under each set of drilling parameters, three holes were made to ensure repeatability. To eliminate the impact of tool wear, each new drill bit was only used for drilling 3 holes and then replaced. The thrust force was measured using a dynamometer (Kistler 9272) coupled with charge amplifier (5070A) and data acquisition unit (5697). The maximum hole wall temperature was captured using a 125 Hz FLIR A6751 thermal camera. It is worth noting that for thrust force measurement and hole delamination damage evaluation, the holes were made near the centre of workpiece. For ease of
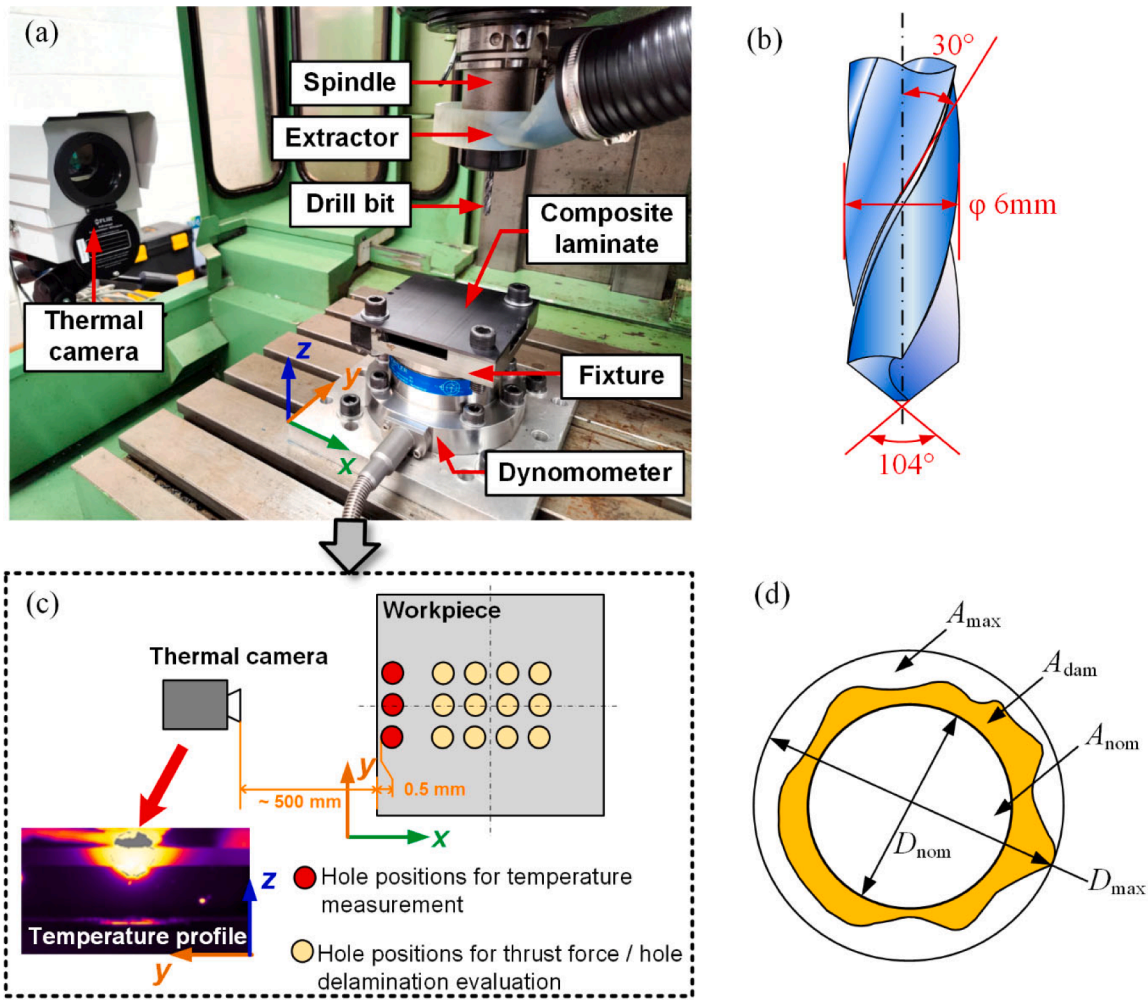
**Fig. 1.** (a) Drilling experiment setup (b) Drill bit geometry (c) Schematic showing the hole positions for temperature and thrust force / hole delamination evaluation (d) Schematic showing the hole delamination damage. (For interpretation of the references to colour in this figure legend, the reader is referred to the web version of this article.)

**Table 1**
Drilling parameters used for the full factorial experiment.

| Level | Spindle speed $S$ [a] (rpm) | | | | Feed rate $F_f$ (mm/rev) | | | | |
|---|---|---|---|---|---|---|---|---|---|
| | 1 | 2 | 3 | 4 | 1 | 2 | 3 | 4 | 5 |
| | 1327 | 2654 | 3981 | 5308 | 0.025 | 0.05 | 0.1 | 0.15 | 0.2 |

[a] 4 levels of spindle speeds $S$ correspond to cutting speed 25, 50, 75, 100 m/min.

temperature measurements, separate holes were drilled 0.5 mm from the composite edge following previous study [37], see Fig. 1 (c).

### 2.1.1. Delamination factor

The drill-out delamination damage images were captured by an Alicona infinite focus microscope and then analysed using Matlab R2021b. The relevant geometric parameters for determining delamination damage are defined in Fig. 1 (d) and delamination factor $F_{da}$ can be calculated following Eqs. (1)–(3) [38]:

$$F_{da} = \alpha \frac{D_{max}}{D_{nom}} + \beta \frac{A_{max}}{A_{nom}} \tag{1}$$

$$\beta = \frac{A_{dam}}{A_{max} - A_{nom}} \tag{2}$$

$$\alpha = 1 - \beta \tag{3}$$

### 2.1.2. Material removal rate

Material removal rate (MRR) describes the material removing efficiency during a machining process and is an important parameter for production efficiency evaluation. The function of MRR ($f_{MRR}$) can be expressed as:

$$f_{MRR}(F_f, S) = \pi R^2 S F_f \tag{4}$$

where R, S, $F_f$ are drill bit radius, spindle speed and feed rate.

### 2.2. Multi-objective optimization

A hybrid multi-objective optimization method combining second-

order polynomial regression, NSGA-II and TOPSIS is deployed here for attaining optimal solutions which balances the trading-off between hole quality metrics and MRR. First, in Section 3, second-order polynomial regression model is used to find the mapping between response variables (thrust force, hole wall temperature and delamination factor $F_{da}$) and machining parameters (feed rate $F_f$ and spindle speed $S$). Then, the optimal non-dominated solutions (Pareto solutions) can be obtained through NSGA-II algorithm in Section 4. Finally, the TOPSIS method is deployed to rank the multiple Pareto solutions according to their proximity to the ideal solution, hence identifying the top-ranking solutions, in Section 5. The flow-chart in Fig. 2 shows the multi-objective optimization procedure in this study.

## 3. Regression model and analysis of variance

To establish the relationships between individual response variables (i.e., thrust force, maximum hole wall temperature $T_{max}$ and delamination factor $F_{da}$) and design variables (i.e., feed rate $F_f$ and spindle speed $S$), a second-order polynomial regression model was established following Eq. (5) [24]:

$$y_m = p_0 + \sum_{i=1}^{k} p_i x_i + \sum_{i=1}^{k} p_{ii} x_i^2 + \sum_{i=1}^{k-1} \sum_{j=2}^{k} p_{ij} x_i x_j \quad (5)$$

where $p_0$, $p_i$, $p_{ii}$, $p_{ij}$ are constants, $x_i$, $x_j$ are independent input drilling parameters and $y_m$ is a response variable for drilling performance evaluation (k = 2 in this case).

ANOVA was deployed to reveal the influence of the drilling parameters on the resulting response variables. Interaction between feed rate $F_f$ and spindle speed $S$ and their second order terms were considered for ANOVA.

### 3.1. Thrust force analysis

Thrust force is considered to be the main reason causing delamination damage as well as hole sub-surface microstructural damage in composite drilling [4], and therefore it should be minimized during optimization for the improved hole quality. Fig. 3 (a) shows the typical thrust force of CF/PEKK and CF/epoxy drilling and the average was taken for the 'stable cutting' phase (between P-I and P-II) for further analysis. The regression function of the thrust force $f_F$ can be expressed as:

$$f_F(F_f, S) = p_0 + p_1 F_f + p_2 S + p_{11} F_f^2 + p_{22} S^2 + p_{12} F_f S \quad (6)$$

where $F_f$ is feed rate, S is spindle speed, $p_0, p_1, p_2, p_{11}, p_{22}$ and $p_{12}$ are the coefficients for the regression model and values are shown in Table 2. The R-Squared ($R^2$) values > 0.85 suggest the satisfactory quality of the regression model [39] and its prediction accuracy will be further verified by experiments in Section 5.

The response surfaces of thrust force for the two composites are
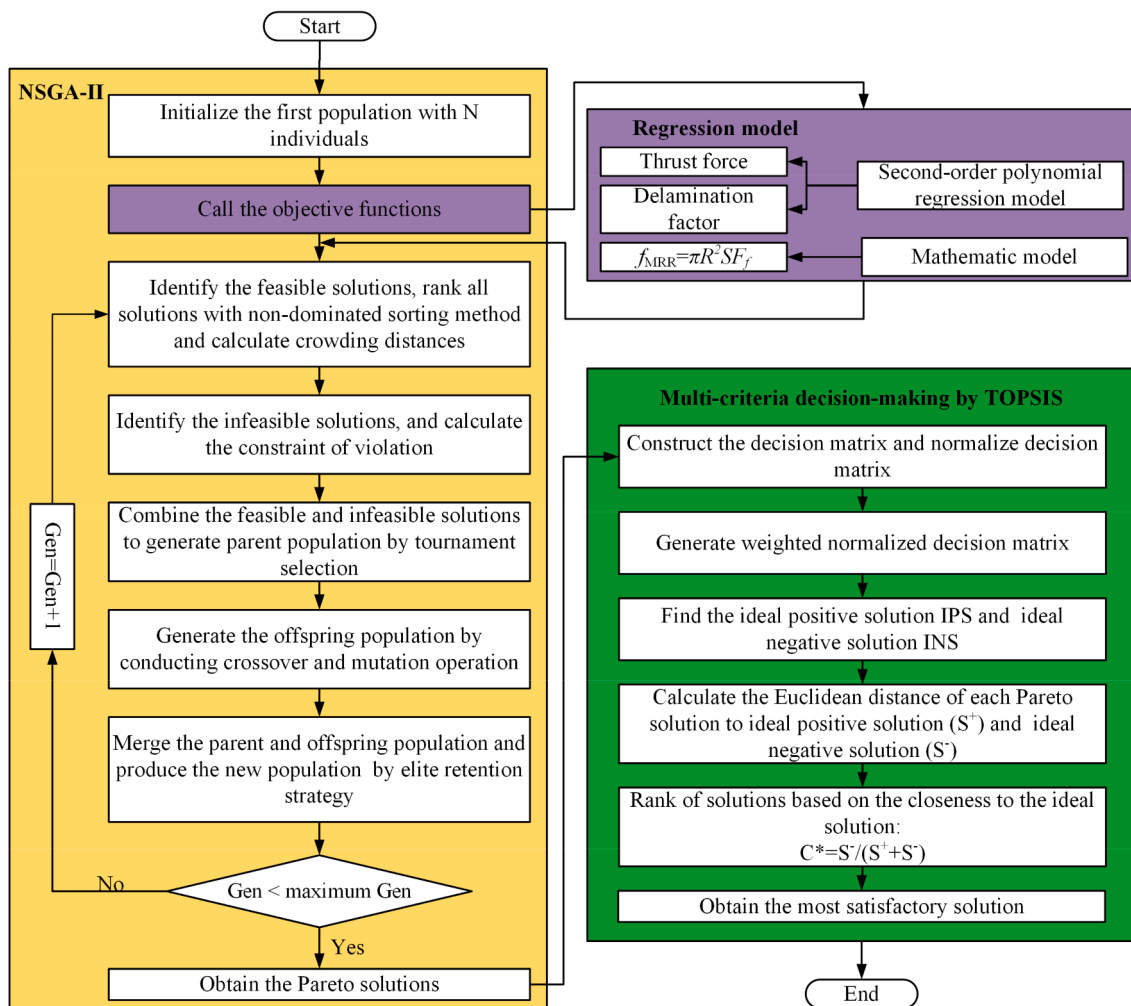


**Fig. 2.** The flow chart of the proposed multi-objective optimization procedure. (For interpretation of the references to colour in this figure legend, the reader is referred to the web version of this article.)
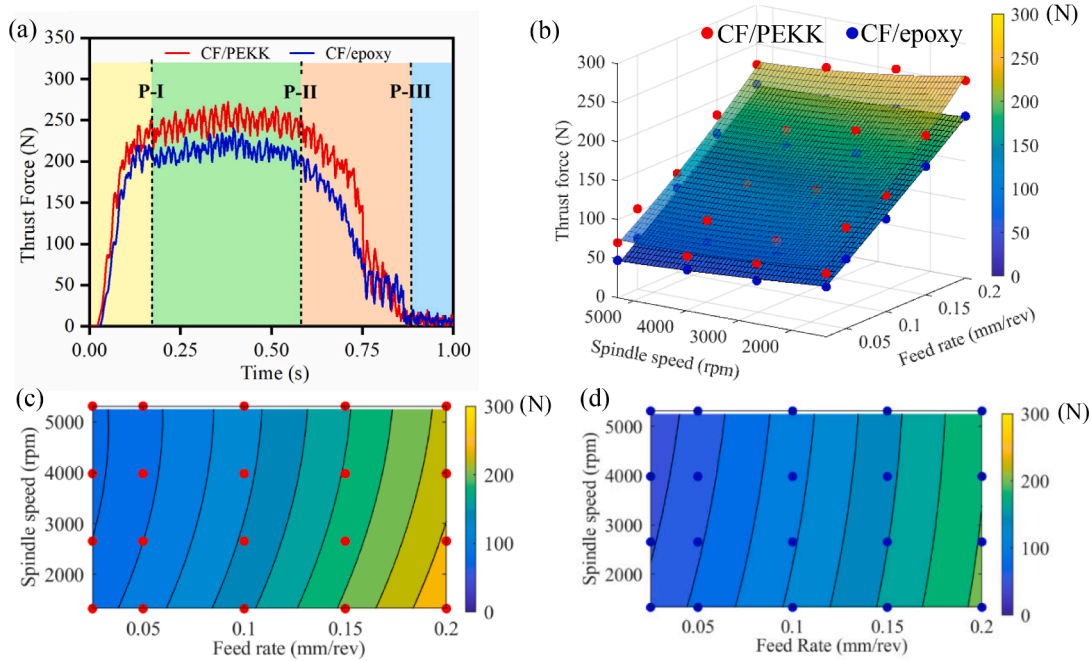
**Fig. 3.** (a) Representative force signals in drilling of the two composites ($F_f = 0.2$ mm/rev, $S = 1327$ rpm); (b) Response surfaces of thrust force of the two composites; (c) Contour of CF/PEKK thrust force with spindle speed and feed rate; (d) Contour of CF/epoxy thrust force with spindle speed and feed rate. (For interpretation of the references to colour in this figure legend, the reader is referred to the web version of this article.)

**Table 2**
Coefficients for regression models of thrust force, $T_{max}$ and $F_{da}$ in drilling of CF/PEKK and CF/epoxy.

| | Material | $p_0$ | $p_1$ | $p_2$ | $p_{11}$ | $p_{22}$ | $p_{12}$ | $R^2$ | RMSE |
|---|---|---|---|---|---|---|---|---|---|
| Thrust force | CF/PEKK | 84.006 | 770.859 | −0.0117 | 995.455 | 1.269E-06 | −0.0232 | 0.986 | 6.988 |
| (N) | CF/epoxy | 54.875 | 746.286 | −0.0073 | 192.897 | 3.803E-07 | 0.0126 | 0.997 | 2.870 |
| $T_{max}$ | CF/PEKK | 165.714 | −1858.864 | 0.0378 | 5728.124 | −5.208E-06 | −0.0013 | 0.892 | 14.881 |
| (°C) | CF/epoxy | 79.386 | −848.354 | 0.0271 | 2608.883 | −3.408E-06 | −0.0125 | 0.884 | 8.197 |
| $F_{da}$ | CF/PEKK | 1.7498 | −10.0782 | −1.9002E-04 | 58.5381 | 3.3064E-08 | −2.2215E-04 | 0.853 | 0.099 |
| | CF/epoxy | 0.9231 | 7.7404 | 6.8357E-06 | 14.2998 | −2.6492E-09 | 3.3268E-05 | 0.907 | 0.227 |

shown in Fig. 3 (b). It is clear that for both composites, the thrust force shows significant increase with feed rate and decreases slightly with spindle speed, see Fig. 3 (c, d). This shows good consistence with the findings reported in drilling of CF/PEEK [18] and CF/epoxy [40]. The drastic increase of thrust force with feed rate can be explained by the considerably increased thickness of material being removed and the slight declining of thrust force with spindle speed could be the result of the thermal softening of matrix under high temperature induced by the enhanced tribological interaction [41]. It is worth mentioning that the thrust force of CF/PEKK is up to ~50 N higher than CF/epoxy. This could be due to the presence of softened and continuous CF/PEKK chips, which are hard to evacuate, hence induced additional resistance at the tool/workpiece interface during drilling [37].

Table 3 shows the ANOVA results for thrust force generation in CF/

PEKK and CF/epoxy respectively. It is clearly evident that for both composites, feed rate is the most influential factor on the thrust force (96.10% contribution for CF/PEKK and 98.72% for CF/epoxy). In comparison, the impact of spindle speed on the thrust force is much lower (1.99% for CF/PEKK vs. 0.92% for CF/epoxy). The second order terms of $F_f$, S and their interaction ($F_f$ S) have negligible influence on the resulting thrust force, with p values > 0.05 being statistically insignificant. The ANOVA results for CF/epoxy drilling showed good consistency with previous studies [24,42,43], where the feed rate is the most influential factor on thrust force (contribution > 85%) while the contribution from the spindle speed was significantly lower (<5%). Despite the vastly different properties of CF/PEKK and CF/epoxy, the contributions of feed rate and spindle speed on the resulting thrust force appear to be at a similar level.

**Table 3**
ANOVA results for thrust force in drilling of CF/PEKK and CF/epoxy.

| Source | CF/PEKK | | | | CF/epoxy | | | |
|---|---|---|---|---|---|---|---|---|
| | Sum of squares | F-value | P-value | Contribution | Sum of squares | F-value | P-value | Contribution |
| $F_f$ | 68797.07 | 986.31 | 2.22E-14 | 96.10% | 56651.14 | 4813.62 | 3.62E-19 | 98.72% |
| S | 1427.83 | 20.47 | 0.000476 | 1.99% | 527.37 | 44.81 | 0.000010 | 0.92% |
| $F_f^2$ | 190.48 | 2.73 | 0.120669 | 0.27% | 7.15 | 0.61 | 0.448615 | 0.01% |
| $S^2$ | 99.84 | 1.43 | 0.251401 | 0.14% | 8.97 | 0.76 | 0.397342 | 0.02% |
| $F_f$ S | 97.37 | 1.40 | 0.257094 | 0.14% | 28.72 | 2.44 | 0.140553 | 0.05% |
| Residual | 976.53 | – | – | 1.36% | 164.76 | – | – | 0.29% |
| Total | 71589.12 | – | – | | 57388.12 | – | – | |

### 3.2. Hole wall temperature

When the drilling temperature exceeds the glass transition temperature ($T_g$) of the polymer matrix, the composite mechanical properties can be significantly degraded and thermal damage can be induced [44]. The highest hole wall temperature was captured when the drill bit cutting edge fully emerged from the workpiece and a typical temperature field image is shown in Fig. 4 (a). The maximum hole wall temperature ($T_{max}$) is used for further analysis in this work. The regression function $f_T$ of $T_{max}$ can be calculated following Eq. (7) and the values of coefficients are shown in Table 2. The R-Squared ($R^2$) values are higher than 0.85, which is considered an indicator of good regression performance [39]. The prediction accuracy will be further verified through experiment validation in Section 5.

$$f_T(F_f, S) = p_0 + p_1 F_f + p_2 S + p_{11} F_f^2 + p_{22} F_f^2 + p_{12} F_f S \qquad (7)$$

The response surfaces of $T_{max}$ of CF/PEKK vs. CF/epoxy are depicted in Fig. 4 (b). For both composites, the maximum hole wall temperature showed a significant decline with feed rate, as high feed rate can reduce the tool-workpiece engagement time and eliminate the heat accumulation effect. It is notable that the $T_{max}$ of CF/PEKK has exceeded/approached the matrix's glass transition temperature ($T_g = 160$ °C) at low feed rate, however the CF/epoxy $T_{max}$ has never exceeded its $T_g$ (130 °C). For both composites, the $T_{max}$ firstly increased and then decreased with the spindle speed. The initial increasing trend can be attributed to the enhanced tribological interaction at high relative speed between the tool and the workpiece [41], which accelerated the frictional heat generation. As the spindle speed further increased, the tool-workpiece contact time was significantly shortened, hence reducing the heat accumulation effect. In comparison with CF/epoxy, the $T_{max}$ of CF/PEKK is up to ~100 °C higher. The drilling induced CF/epoxy chips are mostly in powdery form according to previous studies by Ge et al. [37] and Xu et al. [45]. Due to thermoset epoxy's better thermal stability, the softening of CF/epoxy under machining induced high temperature is rather limited. The fine chips are relatively stiff and can be evacuated efficiently, resulting in minimum chip/tool bit interaction. In contrast, CF/PEKK is highly thermosensitive. The severe softening of the material leads to adhesion of continuous ductile CF/PEKK chip onto the cutting tool. The chips' compliance to the cutting edge results in enlarged tool-chip contact length and generates more frictional heat [37]. Our findings exemplify the strong influence of composite's thermal/mechanical properties on the resulting chip morphology, which consequently affect the drilling induced temperature.

ANOVA results of $T_{max}$ are shown in Table 4. For both CF/PEKK and CF/epoxy, feed rate is still the most influential factor (68.61% and 66.86% contribution, respectively). The second order terms of feed rate start to show increasing significance on the $T_{max}$ (15.42% and 11.28% for CF/PEKK and CF/epoxy, respectively). This means that, the $T_{max}$ is not only affected by feed rate and spindle speed, but also more a complex contribution from other sources (including both first order and second order terms).

### 3.3. Delamination factor analysis

Delamination damage typically occurs at composite hole-exit as a result of Mode-I interlaminar opening fracture [46,47]. The typical binary images of delamination damage in drilling of CF/PEKK and CF/epoxy are shown in Fig. 5 (a) and the delamination damage factor $F_{da}$ are quantified [38]. The regression function $f_D$ of $F_{da}$ can be calculated following Eq. (8) and the values of coefficients are shown in Table 2. R-Squared ($R^2$) values > 0.85 suggest the satisfactory performance of the proposed regression models [39]. The prediction accuracy of the models will be further verified by experimental results.

$$f_D(F_f, S) = p_0 + p_1 F_f + p_2 S + p_{11} F_f^2 + p_{22} S^2 + p_{12} F_f S \qquad (8)$$

The response surfaces for delamination factor $F_{da}$ can be seen in Fig. 5 (b) and it is evident that the $F_{da}$ response surfaces against feed rate and spindle speed are markedly different for the two composites. As
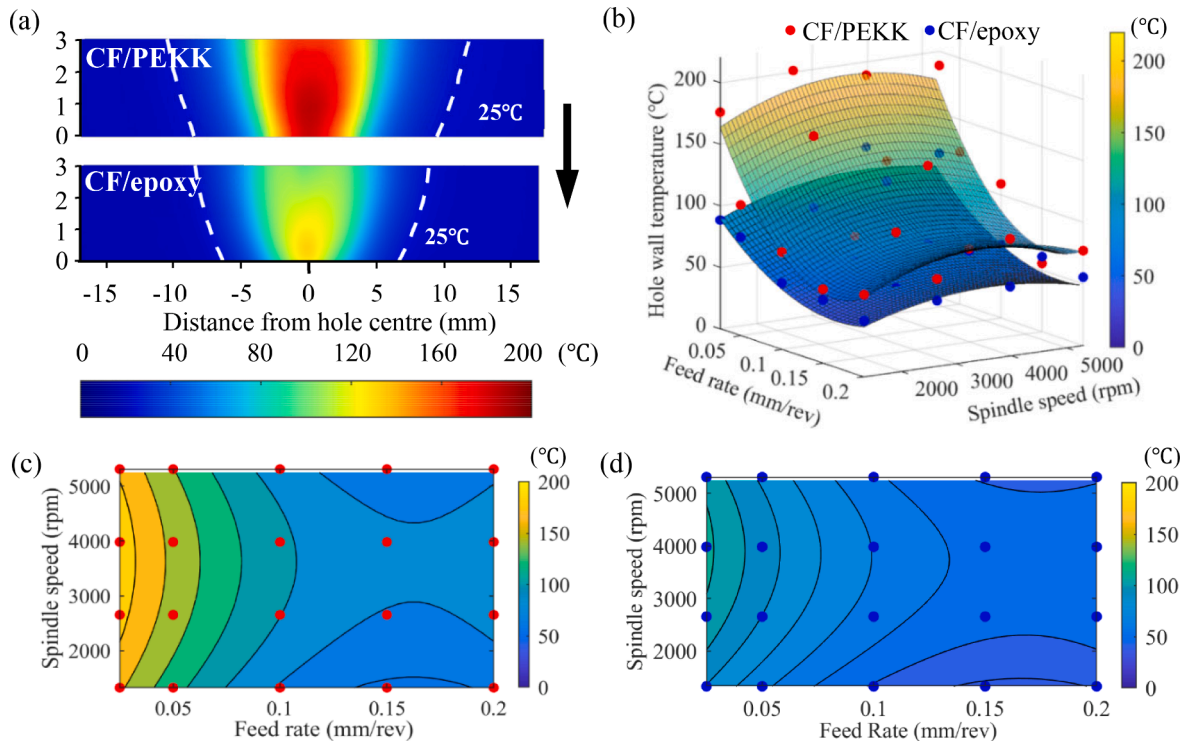


**Fig. 4.** (a) Representative temperature field in drilling of the two composites ($F_f = 0.025$ mm/rev, S = 3981 rpm, black arrow shows the drilling direction; (b) Response surface of $T_{max}$ in drilling of the two composites; (c) Contour of CF/PEKK $T_{max}$ with spindle speed and feed rate (d) Contour of CF/epoxy $T_{max}$ with spindle speed and feed rate. (For interpretation of the references to colour in this figure legend, the reader is referred to the web version of this article.)

**Table 4**
ANOVA results for the maximum hole wall temperature $T_{max}$ in drilling of CF/PEKK and CF/epoxy.

| Source | CF/PEKK | | | | CF/epoxy | | | |
|---|---|---|---|---|---|---|---|---|
| | Sum of squares | F-value | P-value | Contribution | Sum of squares | F-value | P-value | Contribution |
| $F_f$ | 28059.43 | 88.70 | 1.95E-07 | 68.61% | 7758.38 | 80.83 | 3.43E-07 | 66.86% |
| S | 422.17 | 1.33 | 0.267347 | 1.03% | 444.72 | 4.63 | 0.049282 | 3.83% |
| $F_f^2$ | 6307.19 | 19.94 | 0.000534 | 15.42% | 1308.34 | 13.63 | 0.002415 | 11.28% |
| $S^2$ | 1681.78 | 5.32 | 0.036950 | 4.11% | 720.20 | 7.50 | 0.015977 | 6.21% |
| $F_f S$ | 0.33 | 0.001 | 0.974868 | 0.00% | 28.20 | 0.29 | 0.596314 | 0.24% |
| Residual | 4428.95 | – | – | 10.83% | 1343.71 | – | – | 11.58% |
| Total | 40899.84 | – | – | – | 11603.54 | – | – | – |
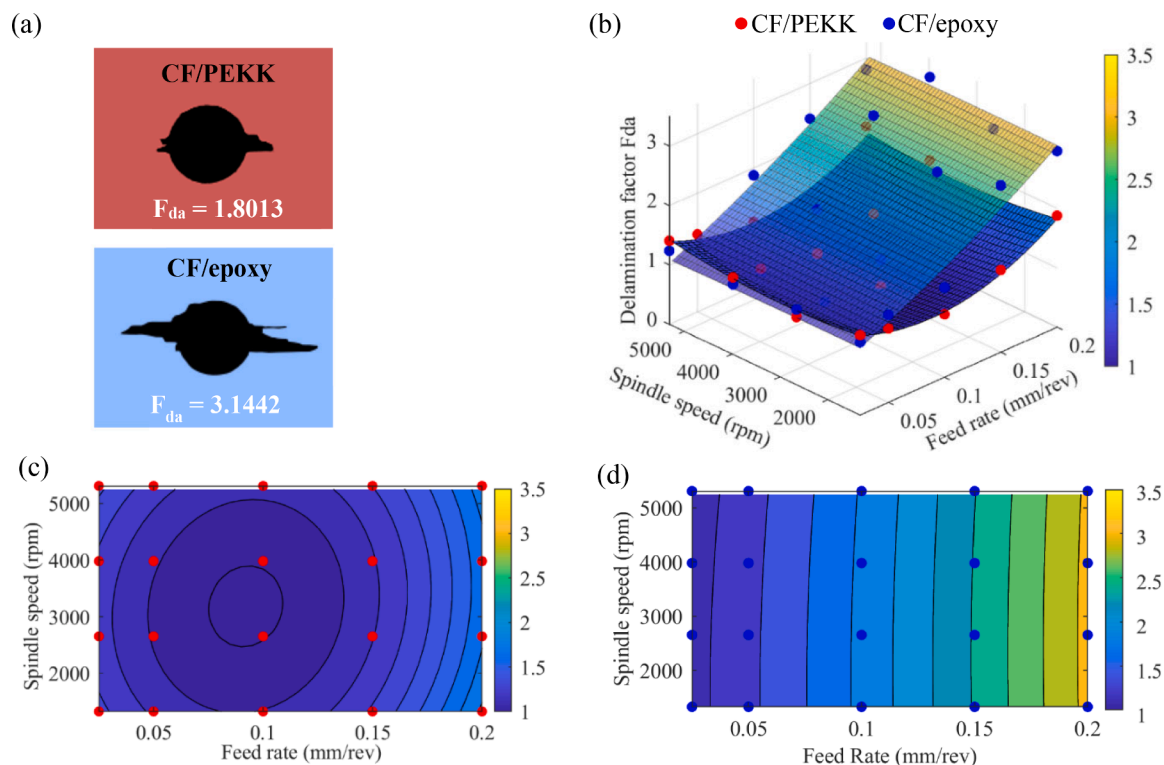


**Fig. 5.** (a) Representative hole delamination damage binary images for CF/PEKK and CF/epoxy ($F_f = 0.2$ mm/rev, S = 1327 rpm); (b) Response surface of delamination factor $F_{da}$ in drilling of two composites; (c) Contour of CF/PEKK delamination factor $F_{da}$ with spindle speed and feed rate; (d) Contour of CF/epoxy delamination factor $F_{da}$ with spindle speed and feed rate. (For interpretation of the references to colour in this figure legend, the reader is referred to the web version of this article.)

shown in Fig. 5 (b-d), $F_{da}$ of CF/PEKK first declines and then grows with both feed rate and spindle speed, while that of CF/epoxy consistently increases with feed rate and is insensitive to spindle speed. This difference can be attributed to the different delamination damage mechanisms of CF/PEKK and CF/epoxy. Delamination damage of CF/PEKK shows typical thermal-mechanical interaction characteristics [37]. Its high drilling temperature (approaching/exceeding the $T_g$) can soften the thermoplastic PEKK matrix and weaken its resistance against deformation. Therefore, under low feed rate ($F_f \leq 0.05$ mm/rev), even the thrust force is quite low, the high drilling temperature (see Fig. 4) can deteriorate the PEKK matrix's stiffness and cause high $F_{da}$. At high feed rate ($F_f \geq 0.1$ mm/rev), the high thrust force (see Fig. 3) takes over the dominance on $F_{da}$ due to Mode-I opening fracture. This explains why $F_{da}$ of CF/PEKK first decreased and then increased with feed rate. In contrast, the delamination damage of CF/epoxy is solely caused by the high thrust force and its mechanical properties are less dependent on temperature. CF/epoxy exhibits more substantial delamination than CF/PEKK, and the largest $F_{da}$ value doubles that of the CF/PEKK. This could be a result of the extremely low interlaminar fracture toughness of CF/epoxy (0.277 N/mm vs. 1.564 N/mm of CF/PEKK) [6,48]. The CF/epoxy

delamination factor $F_{da}$ results reported in this study shows good consistence with the previous work by Davim et al. [49] and Gaitonde et al. [50], where lower feed rate was in favour of reducing delamination damage at hole exit. The significantly different delamination damage seen for CF/PEKK suggests the material would require distinctly different optimal drilling parameters.

Table 5 shows the ANOVA results of $F_{da}$. For CF/PEKK, the second and first order terms of feed rate are the top two influencing factors, with a contribution of 48.79% and 30.72%, respectively. The second order term of spindle speed also has a contribution of 5.02%. This is distinctly different from the results for CF/epoxy, where feed rate is the only significant influencing factor on $F_{da}$ (contribution 90.29%). Our ANOVA results for CF/epoxy are closely in line with the literature [24,51,52], i. e., the feed rate contribution towards $F_{da}$ is greater than 80% and is far higher than the contribution of the spindle speed. Interestingly, drilling of CF/PEKK has led to a drastically different delamination damage variation trend as compared to CF/epoxy. Such discrepancy can be attributed to the thermosensitive nature of CF/PEKK. High delamination at low feed rate may be due to the matrix softening at high machining temperature [53], which weakens the matrix/fibre bonding and hence

**Table 5**
ANOVA results for the $F_{da}$ in drilling of CF/PEKK and CF/epoxy.

| Source | CF/PEKK | | | | CF/epoxy | | | |
|---|---|---|---|---|---|---|---|---|
| | Sum of squares | F-value | P-value | Contribution | Sum of squares | F-value | P-value | Contribution |
| $F_f$ | 0.414689 | 29.26024 | 0.000092 | 30.72% | 9.997926 | 135.567767 | 1.38E-08 | 90.29% |
| S | 0.001601 | 0.11296 | 0.741782 | 0.12% | 0.002313 | 0.031363 | 0.861970 | 0.02% |
| $F_f^2$ | 0.658701 | 46.47758 | 0.000008 | 48.79% | 0.039307 | 0.532985 | 0.477394 | 0.35% |
| $S^2$ | 0.067797 | 4.78373 | 0.046197 | 5.02% | 0.000435 | 0.005902 | 0.939852 | 0.00% |
| $F_f S$ | 0.008908 | 0.62853 | 0.441124 | 0.66% | 0.0002 | 0.002709 | 0.959228 | 0.00% |
| Residual | 0.198414 | – | – | 14.70% | 1.03248 | – | – | 9.32% |
| Total | 1.35011 | – | – | – | 11.072661 | – | – | – |

results in more severe delamination damage.

## 4. Multi-objective optimization

In composite drilling, decreasing thrust force can help suppress the hole wall sub-surface damage and reduce hole-exit delamination damage [4]. As such, minimizing thrust force is considered a way of improving the hole quality. Material removal rate (MRR) on the other hand, characterizes the machining efficiency of the drilling process, hence is preferably maximized. Here, the thrust force, hole-exit delamination damage factor $F_{da}$ and MRR are the three optimization objectives considered in this study and multi-objective optimization is conducted to identify a set of solutions to achieve the global optimization (trade off) between hole quality and the machining efficiency. Additionally, $F_{da}$ and $T_{max}$ should be constrained to ensure the delamination and thermal damage are within an acceptable range [30,35]. The objective functions, constraints and design spaces for the composite drilling optimization can be expressed as follows:

Minimize $(f_F, f_D, -f_{MRR})$

Subject to $0.025 \leq F_f \leq 0.2$

$$1327 \leq S \leq 5308 \tag{9}$$

$f_D \leq 1.4$

$f_T \leq T_g$

where $f_F$, $f_D$, $f_{MRR}$, $f_T$ are functions of thrust force, $F_{da}$, MRR and $T_{max}$, which can be found from Eqs. (4) and (6) - (8). The cutting speed S and feed rate $F_f$ are set to discrete values associated with practical drilling operation [30]. The discrete step size of S is 1 rpm and that for $F_f$ is 0.001 mm/rev.

### 4.1. Multi-objective optimization using NSGA-II algorithm

NSGA-II is an effective algorithm extensively used in multi-objective optimization problems [54]. It uses fast non-dominated sorting approach and crowding distance operator to achieve faster convergence and better population diversity near the Pareto front. More detailed information about the non-dominated sorting approach and crowding distance operator of NSGA-II method deployed in this study can be found in the Supporting information SI.1.

### 4.2. The Pareto front

The Pareto front can be obtained through NSGA-II to best balance the trade-off between the different drilling response variables. The resulting Pareto front can be significantly affected by the size of population (k) and number of iteration (N) used in the algorithm. Therefore, a parametric study is conducted to determine the appropriate k and N and the pareto solutions obtained under different k and N can be found in Support information SI.2 and SI.3. Results show that the pareto solutions

for CF/PEKK are more evenly distributed within the objective space with increasing k and N. For k = 400 and N = 100, a satisfactory distribution of Pareto solutions can be achieved, and the Pareto solutions gradually converged into a true Pareto front. For CF/epoxy, the Pareto solutions showed a much faster convergence with a true Pareto front at k = 100 and N = 30. For fair comparison between CF/PEKK and CF/epoxy, k = 400 and N = 100 were selected for NSGA-II, considering its excellent convergence. The size of cross probability is 0.9 and the mutation probability is set to 1/3, following previous study [30].

The Pareto solutions and corresponding design variables for CF/PEKK and CF/epoxy are shown in Fig. 6. The range of design variables and objective variables covered by the Pareto solutions is visulaized in Fig. 7. For CF/PEKK, the Pareto front consists of 400 Pareto solutions in the objective space, with wide spreading feed rates and spindle speeds in the design space. The design varible ranges are: feed rate 0.036–0.164 mm/rev and spindle speed 2941–5308 rpm. The Pareto solutions covers thrust force ranging from 80.7 to 189.0 N, $F_{da}$ ranging from 1.0000 to 1.4000, and MRR ranging from 4391 to 24564 mm3/min. Such a wide spread of the Pareto solutions resulted in a Pareto front in a 3D surface. In contrast, the Pareto front of CF/epoxy features a single curve in the 3D objective space with only 34 Pareto solutions. Compard to CF/PEKK, the Pareto solutions of CF/epoxy covered a much narrower range (thrust force: 47.3–74.7 N, $F_{da}$: 1.0916 to 1.3920, and MRR: 3750–8700 mm$^3$/min). The corresposning design variables are: feed rate 0.025–0.058 and spindle speed 5308 rpm.

It is worth noting that the spindle speed for CF/epoxy converges to a single value (5308 rpm), the upper limit within design range. This is because, with increasing spindle speed, two of the objectives (MRR and thrust force) evolved to more optimized value (decreased) while $F_{da}$ remained unchanged, see Eq. (4), Fig. 3 (d) and Fig. 5 (d). The highest spindle speed 5308 rpm within the design space can provide both satisfactory hole quality and high drilling efficiency. It is also worth mentioning that the range of feed rate for CF/epoxy is considerably lower than that for CF/PEKK. As indicated by Fig. 5, considering the low interlaminar fracture toughness of CF/epoxy (0.277 N/mm vs. 1.564 N/mm of CF/PEKK [6,48]), the level of feed rate for CF/epoxy has to be restricted in order to ensure $F_{da} < 1.4$. On the other hand, ultilization of low feed rate should be avoided for CF/PEKK drilling due to the poetntial high temperature ($>T_g$) and severe delamination generated by such condition (see Fig. 4 and Fig. 5).

The results suggest that the maximum allowable feed rate of CF/PEKK is 183% higher than that of CF/epoxy, see Fig. 7(a). This correlates to machining efficiency (in terms of MRR) three times greater than that of CF/epoxy, see Fig. 7(e). Although the corresponding maximum thrust force is higher, the resulting $F_{da}$ for CF/PEKK is still within the allowable range, indicating the holes are of satifscatory quality, see Fig. 7(d). The range of thrust force, MRR and $F_{da}$ covered by the Pareto solutions for CF/epoxy in this study is similar to results reported by Wang et al. [30]. However, due to the additional design variable (i.e. tool point angle) envolved in [30], their data features multi-curve plots rather than a single curve feature. By revealing the Pareto front of CF/PEKK drilling and comparing with that of thermoset CF/epoxy, we highlight how different materials properties and their drilliing performance can
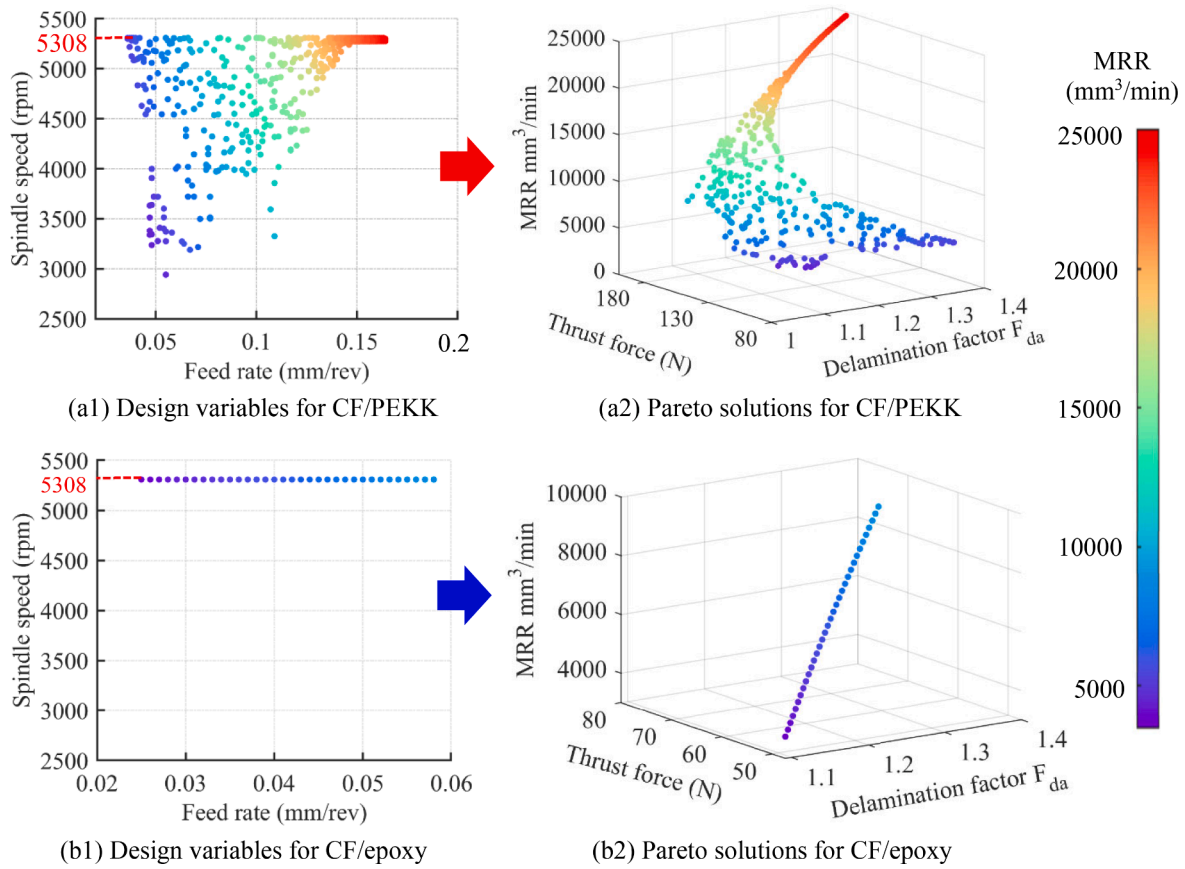
**Fig. 6.** The pareto solutions and corresponding design variables for drilling of CF/PEKK and CF/epoxy. (For interpretation of the references to colour in this figure legend, the reader is referred to the web version of this article.)
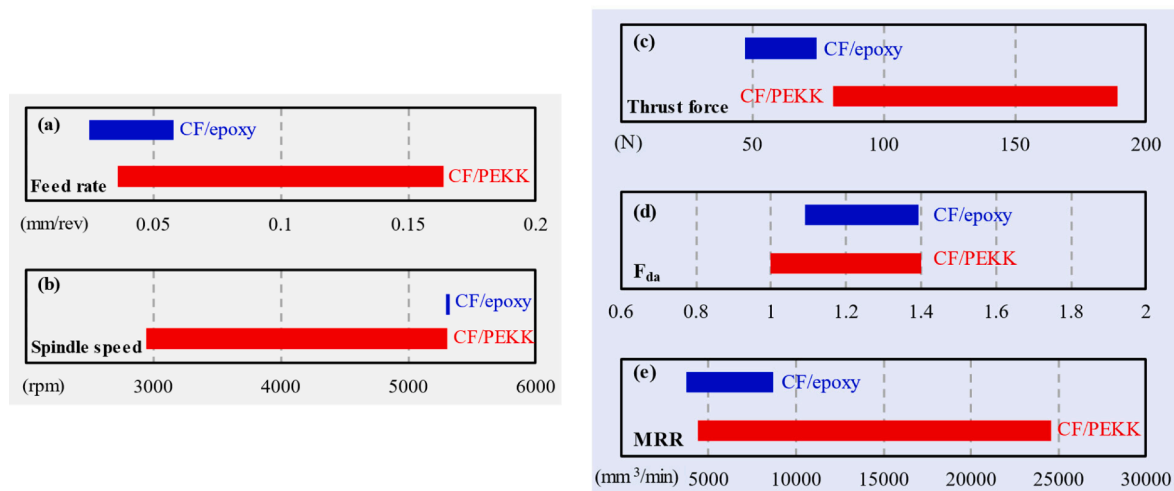


**Fig. 7.** Visualization of the range of (a-b) design variables, and (c-e) objective variables covered by the Pareto solutions. (For interpretation of the references to colour in this figure legend, the reader is referred to the web version of this article.)

influence the ranges of objectives. This further emphasize the importance of considering material properties when conducting future optmization work in relation to composite machining, as the optimization outcome can be highly material property dependent and case sensitive.

Fig. 6 suggests that for CF/epoxy, the improvement of MRR can only be achieved by simultaneously increasing the thrust force and $F_{da}$. This is however, at the price of compromised hole quality. In contrast, for CF/PEKK, the trade-off between the objectives is more complex. To better

reveal the trade-off as well as the correlation between design variables and objectives, a self-organizing map (SOM) is deployed for this work. SOM was previously employed in optimization studies including composite curing [54,55], aerostructure design [56] and social science [57]. In this work, SOM is constructed for the first time in the context of composite machining to visuallize the complex interaction between drilling parameters and drilling performance, see Fig. 8 and Fig. 9. SOM is a type of artificial neural network that is trained by unsupervised competitive learning to create a discretized representation of the input
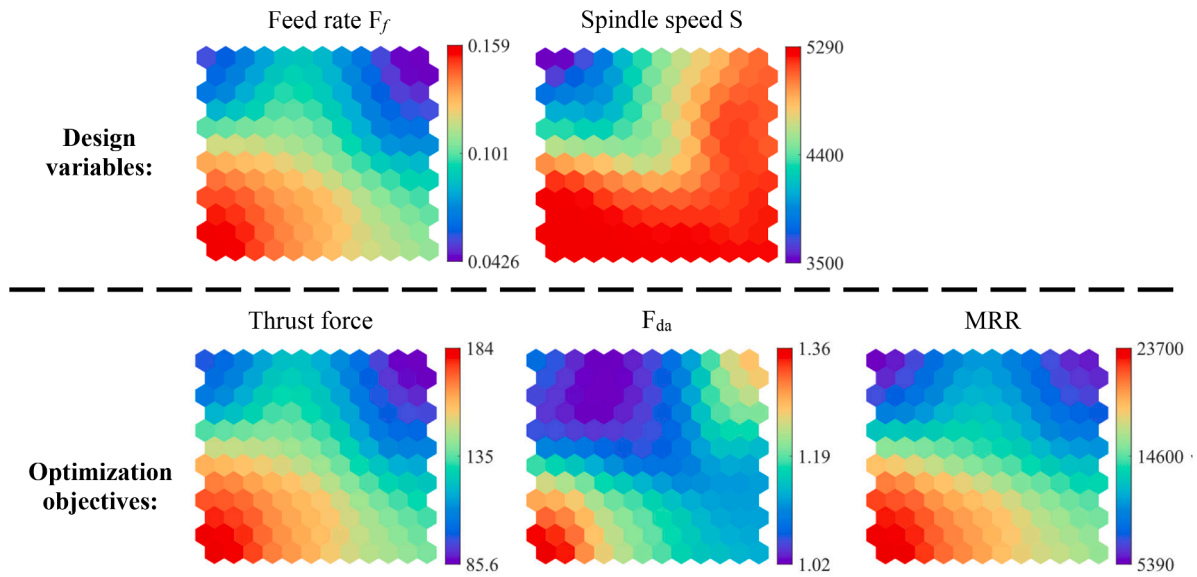
**Fig. 8.** Self-organizing map of the multi-objective optimization results in drilling of CF/PEKK. (For interpretation of the references to colour in this figure legend, the reader is referred to the web version of this article.)
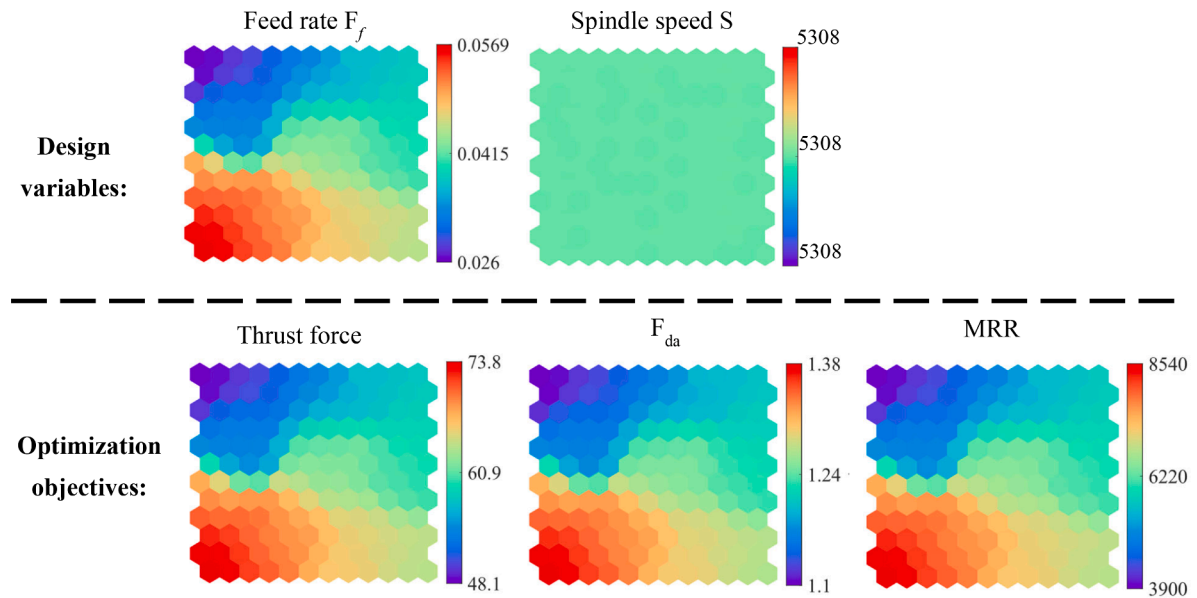


**Fig. 9.** Self-organizing map of the multi-objective optimization results in drilling of CF/epoxy. (For interpretation of the references to colour in this figure legend, the reader is referred to the web version of this article.)

space [54]. $12 \times 12$ neurons were initialized with random weight vector and an initial input vector (including design variables and objectives) was randomly selected from the Pareto solutions. Each node is then examined to calculated the distance between its weight vector and the input vector and hence the Best Matching Unit (BMU) can be obtained. The different values of design variables and objectives are denoted by the different colors and elements in the same position in the maps, and these represent a set of design variables and their corresponding objectives on the Pareto front.

From SOM of CF/PEKK in Fig. 8, it is clear that the feed rate ($F_f$) map has a similar distribution with thrust force and MRR, indicating a positive correlation between the design variable $F_f$ and the two optimization objectives. The effect of feed rate on $F_{da}$ is more complex, as indicated by the different color distribution in the map. It is worth noting that for lower and upper feed rate limit (top right and bottom left of $F_f$ map), relatively high $F_{da}$ can be induced (top right and bottom left of $F_{da}$ map).

For spindle speed, its map showed markly different color distribution with the thrust force, $F_{da}$ and MRR maps. Even at the same level of spindle speed (i.e. the same color region on spindle speed S map), the three objective functions can vary significantly, indicating spindle speed has no significant influence on the three objectives. On the other hand, the optimizaton objective maps for thrust force and MRR have similar color distribution, this implies increasing the CF/PEKK MRR can only be achieved at the cost of increased thrust force. The trade-off between $F_{da}$ and MRR is non-monotonic, considering their significantly different color distribution. However, it is worth noting that the maximum MRR can only be achived with the highest $F_{da}$ (see bottom left of MRR and $F_{da}$ maps).

For SOM of CF/epoxy in Fig. 9, the map of feed rate is similar to all the three objective maps, indicating a strong positive correlation between the feed rate and the objectives. The single color spindle speed map is consistent with the converged single value (5308 rpm) obtained

from the Pareto solutions.

*4.3. Convergence evaluation*

The convergence of the optimization is evaluated using the average values of the objectives in the Pareto solutions [51], see results in Supporting information SI 4. The average thrust force, $F_{da}$ and MRR stabilize at the 20th generation for CF/PEKK and the 10th generation for CF/epoxy. The different levels of average objectives between CF/PEKK and CF/epoxy are consistent with results in Fig. 6. Therefore, the Pareto solutions obtained for the 100th generation is deemed reliable in this study.

**5. Decision making based on TOPSIS and verification**

The Pareto solutions obtained from Section 4 contain a large number of optimal solutions. However, for practical composite drilling, a specific set of drilling parameters should be identified from the Pareto solutions [51], and this can be achieved by ranking all the available alternatives through MCDM. In this study, TOPSIS is deployed to rank the Pareto solutions based on the distance of one solution to the ideal positive solution (IPS) and ideal negative solution (INS) [33]. The distances are defined as $S_i^+$ and $S_i^-$, respectively. The overall performance index $C_i^*$ of each Pareto solution based on its proximity to the ideal solution can be calculated by:

$$C_i^* = \frac{S_i^-}{S_i^+ + S_i^-} (i = 1, 2, ..., m) \tag{10}$$

where $0 \leq C_i^* \leq 1$ with $C_i^*$ approaching 1 deemed a better performance index. More detailed procedures for the TOPSIS method can be found in Supporting information SI.5.

The ranking of the Pareto solutions for CF/PEKK and CF/epoxy can be found in Fig. 10. The most satisfactory solutions (Rank1) are summarized in Table 6. Two composites showed the same optimal spindle speed (5308 rpm), but the optimal feed rate ($F_f = 0.144$ mm/rev) of CF/PEKK is 152.6% higher than that of CF/epoxy. The different optimal drilling parameters obtained for the two composites can be attributed to the disparate drilling performance as a result of their distinctly different mechical and thermal properties. CF/PEKK delamination damage is highly sensitive to temperature (especially when approaching/ exceeding $T_g$). This can soften the composite plies and deteriorate their resistance against bending-induced interlaminar fracture [4]. Therefore, low feed rate that leads to severe heat accomulation should be avoided for CF/PEKK, as indicated by Fig. 4. For CF/epoxy on the other hand, the delamination damage is more sensitive to high thrust force (due to its low Mode-I interlaminar fracture toughness [48]), but less susceptible to high temperature as shown in Fig. 5. As such, high feed rate should be avoid for CF/epoxy in order to minimize severe delamination damage. Under the optimized drilling conditions, although CF/PEKK generates 134% higher thrust force than CF/epoxy, it can still achieve satisfactory hole quality with acceptable delamination damage ($F_{da} < 1.4$) and 13.5% lower maximum hole wall temperature. Most importantly, CF/PEKK shows more superior machinability as compared to CF/epoxy, with 152.6 % higher MRR.

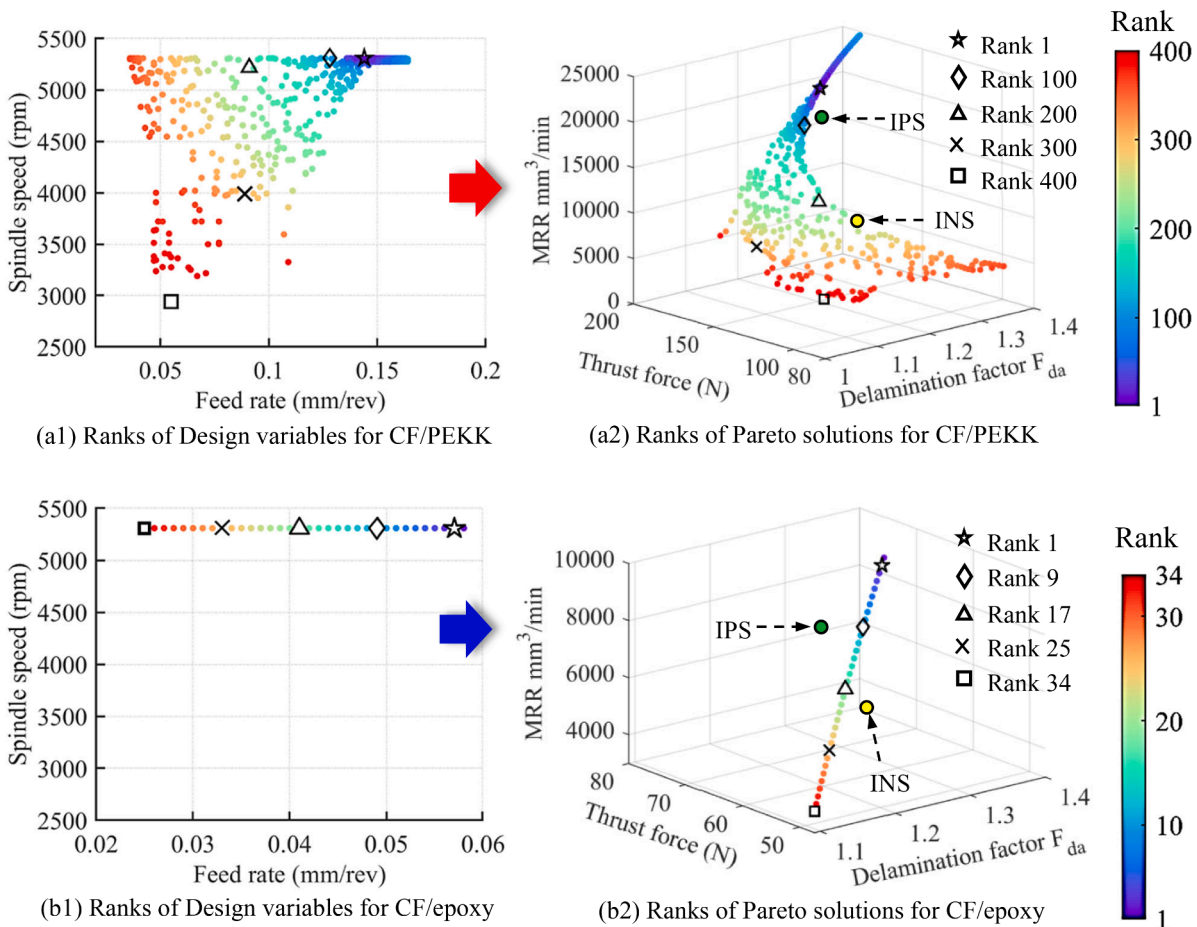To verify the accuracy of our regression model, five representative



**Fig. 10.** Ranks of Pareto solutions obtained by TOPSIS and the corresponding design variables for drilling of CF/PEKK and CF/epoxy. (For interpretation of the references to colour in this figure legend, the reader is referred to the web version of this article.)

**Table 6**

The top-ranking solutions identified by TOPSIS for CF/PEKK and CF/epoxy.

| Materials | Design variables | | Objectives (experimental value) | | | Maximum hole wall temperature $T_{max}$(°C) |
|---|---|---|---|---|---|---|
| | Feed rate (mm/rev) | Spindle speed (rpm) | Thrust force (N) | Delamination factor $F_{da}$ | MRR (mm$^3$/min) | |
| CF/PEKK | 0.144 | 5308 | 159.8 | 1.2350 | 21,601 | 67.8 |
| CF/epoxy | 0.057 | 5308 | 68.3 | 1.2703 | 8550 | 78.4 |

solutions with different rankings were selected for CF/PEKK and CF/epoxy respectively for experimental validation, and the predicted and experimental values of thrust force, $F_{da}$ and $T_{max}$ are summarized in Table 7 and Table 8. For CF/PEKK, the mean relative errors between experimental and predicted results are 5.6% for thrust force, 6.0% for delamination factor $F_{da}$, and 4.6% for maximum hole wall temperature. For CF/epoxy, the associated errors are 4.3%, 7.6%, and 8.5%, respectively. The small range of errors in our validation results is comparable to previous published CFRP drilling studies [30,58], implying the acceptable prediction accuracy of our second-order regression model. Through multi-objective optimization using the proposed hybrid method, $T_{max}$ and delamination damage can be well constrained to eliminate excessive thermal and hole delamination damage.

The validity of the multi-objective optimization is further verified by evaluating the performance index $C_i^*$ in Table 7 and Table 8. The top-ranking solutions correlate to the highest $C_i^*$ value (closest to 1) from the experiment verification, confirming the validity of the parameter ranking. To demonstrate the advantage of our multi-objective optimal solutions over single-objective-best solutions, $C_i^*$ values were also compared for both scenarios, see Table 9. It can be seen that compared to single-objective-best solutions, $C_i^*$ of the multi-objective optimal solutions can achieve 13.4%–67.6% performance improvement for CF/PEKK and 29.6%−83.3% improvement for CF/epoxy. Compared to previous studies where the optimization problem was dealt by converting multi-objective problem into a single-objective one [24,25,26], our approach shows better robustness and reliability. The complex trade-off relationship between multiple objectives can be effectively visualized and the best closeness to the ideal solution (with optimal values of all objectives) can be achieved. This means the proposed new approach not only achieved better trade-off between different objectives, but also attained the optimal closeness to the ideal solution.

## 6. Conclusions

This paper reports the first multi-objective optimization for carbon fibre reinforced thermoplastic (CFRTP) drilling. A hybrid optimization algorithm integrating Non-dominated Sorting Genetic Algorithm-II (NSGA-II) and Techniques for Order of Preference by Similarity to Ideal Solution (TOPSIS) is proposed for drilling of CF/PEKK, with the aim of accurately predicting the composite's drilling performance, obtaining the Pareto optimal solutions and ranking the multiple alternatives based on their proximity to ideal solutions. This work also presents the first comparative study on the optimal drilling conditions of thermoplastic CF/PEKK and thermoset CF/epoxy, to reveal the impact of composite matrix thermal-mechanical properties / machining performance on the final optimization outcome. By deploying the more

sustainable CF/PEKK composite and enhancing its manufacturing efficiency, we believe this work will have a long-lasting impact on sustainable manufacturing of next generation composites and contribute to a greener aviation industry. This study will not only provide important parametric guidance for sustainable manufacturing of next generation CFRTP but will inspire new lines of research such as development of novel CFRTP cutting tools and predictive machining damage models for CFRTP. The main conclusions and future recommendations are as follows:

- Thermoplastic CF/PEKK and thermoset CF/epoxy showed similar ANOVA results for thrust force and maximum hole wall temperature, with feed rate being the most influential factor (contribution >95% for thrust force and >65% for hole wall temperature). However, ANOVA results for delamination factor suggested that the second order term of feed rate was the most influential factor for CF/PEKK delamination damage (48.8% contribution), whereas the first order term of feed rate dominated the delamination of CF/epoxy (90.3% contribution). Such difference can be attributed to the thermoplastic nature of CF/PEEK and its distinctly different thermal-mechanical properties as compared to CF/epoxy.

- When compared with CF/epoxy, CF/PEKK drilling generated up to ~50 N higher thrust force, ~100 °C higher maximum hole wall temperature, but significantly lower delamination damage. This is related to the different chip formation mechanisms of CF/PEKK, the associated tool/chip/workpiece interaction, as well as the material's high Mode-I interlaminar fracture toughness.

- The second-order polynomial regression model can well predict the thrust force, maximum hole wall temperature and delamination damage factor of both CF/PEKK and CF/epoxy (4.3%−8.5% relative error). With the proposed hybrid optimization method, Pareto solutions which meet the temperature/delamination constraints have been identified and the overall optimized performance with trade-off between hole quality and production efficiency has been achieved. The complex interaction between the design varibles and the objectives in composite drilling was visulaized for the first time through self-organizing map. By revealing the Pareto front of CF/PEKK drilling and comparing with that of thermoset CF/epoxy, we revealed the impact of different matrix properties on the composites drilling performance, which subsequently influence the ranges of optimal objectives.

- With proper ranking of multiple Pareto solutions through TOPSIS, the most satisfactory solutions identified for CF/PEKK are: feed rate = 0.144 mm/rev and spindle speed = 5308 rpm; and for CF/epoxy: feed rate = 0.057 mm/rev and spindle speed = 5308 rpm. This verifies the necessity of considering composite matrix thermal-

**Table 7**

Predicted and experimental values of thrust force, $F_{da}$, $T_{max}$ and relative errors in CF/PEKK.

| Rank | Feed rate (mm/rev) | Spindle speed (rpm) | Thrust force (N) | | | Delamination factor $F_{da}$ | | | $T_{max}$ (°C) | | | Performance index $C_i^*$ |
|---|---|---|---|---|---|---|---|---|---|---|---|---|
| | | | Pre | Exp | Error | Pre | Exp | Error | Pre | Exp | Error | |
| 1 | 0.144 | 5308 | 170.1 | 159.8 | 6.4% | 1.2655 | 1.2350 | 2.5% | 69.7 | 67.8 | 2.7% | 0.6414 |
| 100 | 0.128 | 5308 | 155.4 | 148.1 | 5.0% | 1.1909 | 1.0839 | 9.8% | 74.6 | 71.6 | 4.2% | 0.6325 |
| 200 | 0.091 | 5217 | 123.4 | 117.7 | 4.8% | 1.1206 | 1.0532 | 6.4% | 98.8 | 95.5 | 3.4% | 0.5207 |
| 300 | 0.089 | 3990 | 124.7 | 120.5 | 3.4% | 1.0059 | 1.0727 | 6.2% | 113.1 | 110.0 | 2.8% | 0.4085 |
| 400 | 0.055 | 2941 | 101.4 | 93.2 | 8.6% | 1.0638 | 1.1205 | 5.1% | 146.7 | 133.4 | 9.9% | 0.3622 |
| Error (Ave) | – | | | | 5.6% | – | | 6.0% | – | | 4.6% | – |

**Table 8**
Predicted and experimental values of thrust force, $F_{da}$, $T_{max}$ and relative errors in CF/epoxy.

| Rank | Feed rate (mm/rev) | Spindle speed (rpm) | Thrust force (N) | | | Delamination factor $F_{da}$ | | | $T_{max}$ (°C) | | | Performance index $C_i^*$ |
|------|------|------|------|------|------|------|------|------|------|------|------|------|
| | | | Pre | Exp | Error | Pre | Exp | Error | Pre | Exp | Error | |
| 1 | 0.057 | 5308 | 73.8 | 68.3 | 8.1% | 1.3824 | 1.2703 | 8.8% | 83.6 | 78.4 | 6.6% | 0.6729 |
| 10 | 0.049 | 5308 | 67.1 | 65.2 | 3.0% | 1.3070 | 1.1992 | 9.0% | 88.6 | 81.2 | 9.1% | 0.6201 |
| 18 | 0.041 | 5308 | 65.5 | 61.2 | 7.0% | 1.2334 | 1.1355 | 8.6% | 94.1 | 86.9 | 8.3% | 0.5115 |
| 26 | 0.033 | 5308 | 53.9 | 54.0 | 2.5% | 1.1616 | 1.1630 | 0.1% | 99.9 | 91.4 | 9.3% | 0.4162 |
| 34 | 0.025 | 5308 | 47.3 | 47.8 | 1.1% | 1.0916 | 1.2390 | 11.9% | 105.9 | 117.1 | 9.5% | 0.3673 |
| Error(Ave) | – | | | | 4.3% | – | | 7.6% | | | 8.5% | – |

**Table 9**
Performance indices ($C_i^*$) for multi-objective optimal solution and single-objective optimal solutions in CF/PEKK and CF/epoxy.

| Optimal solutions | CF/PEKK | | | CF/epoxy | | |
|------|------|------|------|------|------|------|
| | Feed rate (mm/rev) | Spindle speed (rpm) | $C_i^*$ | Feed rate (mm/rev) | Spindle speed (rpm) | $C_i^*$ |
| Multi-objective by TOPSIS | 0.144 | 5308 | 0.6414 | 0.057 | 5308 | 0.6729 |
| Single best - thrust force | 0.025 | 5308 | 0.3828 | 0.025 | 5308 | 0.3670 |
| Single best - delamination factor | 0.109 | 3325 | 0.3670 | 0.025 | 5308 | 0.3958 |
| Single best - MRR | 0.2 | 5308 | 0.5657 | 0.2 | 5308 | 0.5192 |

mechanical properties when conducting future optimization work in composite machining, as the optimization outcome can be highly material property dependent and case sensitive.

- Under the optimal drilling parameters, CF/PEKK generates 134% higher thrust force than CF/epoxy. However, it can still achieve satisfactory hole quality (delamination damage factor $F_{da} < 1.4$) and 13.5% lower maximum hole wall temperature. Most importantly, CF/PEKK shows more superior machinability with 152.6 % higher machining efficiency as compared to CF/epoxy.
- Future work would benefit from more advanced mathematical/numerical models that consider temperature effects on the hole quality/damage. Also, additional metrics for hole quality evaluation (e.g. burr formation, hole geometrical accuracy and hole wall microstructure/surface roughness) and tool wear may be considered as optimization objectives in future research, to better control the machining quality.

*CRediT authorship contribution statement*

**Jia Ge:** Conceptualization, Methodology, Investigation, Writing – original draft. **Wenchang Zhang:** Methodology, Investigation, Writing – review & editing. **Ming Luo:** Resources, Writing – review & editing. **Giuseppe Catalanotti:** Supervision, Writing – review & editing. **Brian G. Falzon:** Writing – review & editing. **Colm Higgins:** Resources, Writing – review & editing. **Dinghua Zhang:** Resources, Writing – review & editing. **Yan Jin:** Supervision, Writing – review & editing, Funding acquisition, Project administration. **Dan Sun:** Conceptualization, Methodology, Investigation, Writing – review & editing, Funding acquisition, Project administration.

**Declaration of Competing Interest**

The authors declare that they have no known competing financial interests or personal relationships that could have appeared to influence the work reported in this paper.

**Data availability**

Data will be made available on request.

**Acknowledgement**

**Appendix A. Supplementary data**

Supplementary data to this article can be found online at https://doi.org/10.1016/j.compositesa.2022.107418.

**References**

[1] Davim JP. Computational methods and production engineering: research and development. Woodhead Publishing; 2017.

[2] Marinosci VM, Chu L, Grouve WJB, Wijskamp S, Akkerman R, de Rooij MB. Characterization of the water–titanium interaction and its effect on the adhesion of titanium-C/PEKK joints. Compos Part A Appl Sci Manuf 2022;162:107107. https://doi.org/10.1016/j.compositesa.2022.107107.

[3] Pérez-Martín H, Mackenzie P, Baidak A, Ó Brádaigh CM, Ray D. Crystallisation behaviour and morphological studies of PEKK and carbon fibre/PEKK composites. Compos Part A Appl Sci Manuf 2022;159:106992. https://doi.org/10.1016/j.compositesa.2022.106992.

[4] Ge J, Catalanotti G, Falzon BG, McClelland J, Higgins C, Jin Y, et al. Towards understanding the hole making performance and chip formation mechanism of thermoplastic carbon fibre/polyetherketoneketone composite. Compos Part B Eng 2022;109752. https://doi.org/10.1016/j.compositesb.2022.109752.

[5] Krishnaraj V, Zitoune R, Davim JP. Drilling of polymer-matrix composites. Springer; 2013.

[6] Tan W, Falzon BG, Chiu LNS, Price M. Predicting low velocity impact damage and Compression-After-Impact (CAI) behaviour of composite laminates. Compos Part A Appl Sci Manuf 2015;71:212–26. https://doi.org/10.1016/j.compositesa.2015.01.025.

[7] Davim JP, Reis P. Machinability study on composite (polyetheretherketone reinforced with 30% glass fibre–PEEK GF 30) using polycrystalline diamond (PCD) and cemented carbide (K20) tools. Int J Adv Manuf Technol 2004;23:412–8. https://doi.org/10.1007/s00170-003-1779-7.

[8] Heo Y, Sodano HA. Thermally responsive self-healing composites with continuous carbon fiber reinforcement. Compos Sci Technol 2015;118:244–50. https://doi.org/10.1016/j.compscitech.2015.08.015.

[9] Yao S-S, Jin F-L, Rhee KY, Hui D, Park S-J. Recent advances in carbon-fiber-reinforced thermoplastic composites: A review. Compos Part B Eng 2018;142:241–50. https://doi.org/10.1016/j.compositesb.2017.12.007.

[10] Bonmatin M, Chabert F, Bernhart G, Cutard T, Djilali T. Ultrasonic welding of CF/PEEK composites: Influence of welding parameters on interfacial temperature profiles and mechanical properties. Compos Part A Appl Sci Manuf 2022;162:107074. https://doi.org/10.1016/j.compositesa.2022.107074.

[11] Davim JP. Machining composites materials. John Wiley & Sons; 2013.

[12] Davim JP. Machining: fundamentals and recent advances; 2008.

[13] Meinhard D, Haeger A, Knoblauch V. Drilling induced defects on carbon fiber-reinforced thermoplastic polyamide and their effect on mechanical properties. Compos Struct 2021;256:113138. https://doi.org/10.1016/j.compstruct.2020.113138.

[14] Ge J, Reji R, Feist T, Elmore A, McClelland J, Higgins C, et al. Investigating hole making performance of Al 2024–T3/Ti-6Al-4V alloy stacks: A comparative study of conventional drilling, peck drilling and helical milling. Int J Adv Manuf Technol 2022;120:5027–40. https://doi.org/10.1007/s00170-022-09062-x.

[15] Campos Rubio J, Abrao AM, Faria PE, Correia AE, Davim JP. Effects of high speed in the drilling of glass fibre reinforced plastic: Evaluation of the delamination factor. Int J Mach Tools Manuf 2008;48:715–20. https://doi.org/10.1016/j.ijmachtools.2007.10.015.

[16] Kakinuma Y, Ishida T, Koike R, Klemme H, Denkena B, Aoyama T. Ultrafast feed drilling of carbon fiber-reinforced thermoplastics. Procedia CIRP 2015;35:91–5. https://doi.org/10.1016/j.procir.2015.08.074.

[17] Ferreira Batista M, Basso I, de Assis TF, Roger Rodrigues A, Ricardo TJ. Cryogenic drilling of carbon fibre reinforced thermoplastic and thermoset polymers. Compos Struct 2020;251:112625. https://doi.org/10.1016/j.compstruct.2020.112625.

[18] Xu J, Huang X, Davim JP, Ji M, Chen M. On the machining behavior of carbon fiber reinforced polyimide and PEEK thermoplastic composites. Polym Compos 2020;41:3649–63. https://doi.org/10.1002/pc.25663.

[19] Gaugel S, Sripathy P, Haeger A, Meinhard D, Bernthaler T, Lissek F, et al. A comparative study on tool wear and laminate damage in drilling of carbon-fiber reinforced polymers (CFRP). Compos Struct 2016;155:173–83. https://doi.org/10.1016/j.compstruct.2016.08.004.

[20] Davim JP, Mata F, Gaitonde VN, Karnik SR. Machinability evaluation in unreinforced and reinforced PEEK composites using response surface models. J Thermoplast Compos Mater 2010;23:5–18. https://doi.org/10.1177/0892705708093503.

[21] Ge J, Tan W, Catalanotti G, Falzon BG, McClelland J, Higgins C, Jin Y, Sun D. Understanding chip formation in orthogonal cutting of thermoplastic CF/PEKK composites based on finite element method. In: Shafik M, Case K, editors. Adv. Manuf. Technol. Proc. 19th Int. Conf. Manuf. Res. Inc. 36th Natl. Conf. Manuf. Res., vol. 25, IOS Press; 2022, p. 161–6. 10.3233/ATDE220584.

[22] Davim JP, Aveiro P. Design of experiments in production engineering. Springer; 2016.

[23] Davim JP. Statistical and computational techniques in manufacturing. Springer Science & Business Media; 2012.

[24] Feito N, Muñoz-Sánchez A, Díaz-Álvarez A, Miguelez MH. Multi-objective optimization analysis of cutting parameters when drilling composite materials with special geometry drills. Compos Struct 2019;225:111187. https://doi.org/10.1016/j.compstruct.2019.111187.

[25] Feito N, Milani AS, Muñoz-Sánchez A. Drilling optimization of woven CFRP laminates under different tool wear conditions: a multi-objective design of experiments approach. Struct Multidiscip Optim 2016;53:239–51. https://doi.org/10.1007/s00158-015-1324-y.

[26] Soepangkat BOP, Norcahyo R, Effendi MK, Pramujati B. Multi-response optimization of carbon fiber reinforced polymer (CFRP) drilling using back propagation neural network-particle swarm optimization (BPNN-PSO). Eng Sci Technol an Int J 2020;23:700–13. https://doi.org/10.1016/j.jestch.2019.10.002.

[27] Abhishek K, Datta S, Mahapatra SS. Multi-objective optimization in drilling of CFRP (polyester) composites: Application of a fuzzy embedded harmony search (HS) algorithm. Measurement 2016;77:222–39. https://doi.org/10.1016/j.measurement.2015.09.015.

[28] Ng LY, Chemmangattuvalappil NG, Dev VA, Eden MR. Chapter 1 - Mathematical principles of chemical product design and strategies. In: Martín M, Eden MR, Chemmangattuvalappil NG, editors. Tools Chem. Prod. Des., vol. 39, Elsevier; 2016, p. 3–43. https://doi.org/10.1016/B978-0-444-63683-6.00001-0.

[29] Sardiñas RQ, Reis P, Davim JP. Multi-objective optimization of cutting parameters for drilling laminate composite materials by using genetic algorithms. Compos Sci Technol 2006;66:3083–8. https://doi.org/10.1016/j.compscitech.2006.05.003.

[30] Wang Q, Jia X. Multi-objective optimization of CFRP drilling parameters with a hybrid method integrating the ANN. NSGA-II and fuzzy C-means Compos Struct 2020;235:111803. https://doi.org/10.1016/j.compstruct.2019.111803.

[31] Wang Z, Rangaiah GP. Application and Analysis of Methods for Selecting an Optimal Solution from the Pareto-Optimal Front obtained by Multiobjective Optimization. Ind Eng Chem Res 2017;56:560–74. https://doi.org/10.1021/acs.iecr.6b03453.

[32] Hwang C-L, Yoon K. Methods for Multiple Attribute Decision Making. Mult. Attrib. Decis. Mak. Methods Appl. A State-of-the-Art Surv., Berlin, Heidelberg: Springer Berlin Heidelberg; 1981, p. 58–191. 10.1007/978-3-642-48318-9_3.

[33] Li N, Sheikh-Ahmad JY, El-Sinawi A, Krishnaraj V. Multi-objective optimization of the trimming operation of CFRPs using sensor-fused neural networks and TOPSIS. Measurement 2019;132:252–62. https://doi.org/10.1016/j.measurement.2018.09.057.

[34] Jadhav PS, Mohanty CP, Hotta TK, Gupta M. An optimal approach for improving the machinability of Nimonic C-263 superalloy during cryogenic assisted turning. J Manuf Process 2020;58:693–705. https://doi.org/10.1016/j.jmapro.2020.08.017.

[35] Liu L, Qu D, Cao H, Huang X, Song Y, Kang X. Process optimization of high machining efficiency and low surface defects for HSD milling UD-CF/PEEK with

[36] Tan W, Falzon BG, Price M, Liu H. The role of material characterisation in the crush modelling of thermoplastic composite structures. Compos Struct 2016;153:914–27. https://doi.org/10.1016/j.compstruct.2016.07.011.

[37] Ge J, Luo M, Zhang D, Catalanotti G, Falzon BG, Mcclelland J, Jin Y, Sun D. Temperature field evolution and thermal-mechanical interaction induced damage in drilling of thermoplastic CF/PEKK – A comparative study with thermoset CF/epoxy. ChemRxiv Cambridge Cambridge Open Engag 2022:1–32. 10.26434/chemrxiv-2022-6rxx8.

[38] Davim JP, Rubio JC, Abrao AM. A novel approach based on digital image analysis to evaluate the delamination factor after drilling composite laminates. Compos Sci Technol 2007;67:1939–45. https://doi.org/10.1016/j.compscitech.2006.10.009.

[39] Shu L, Li S, Fang Z, Kizaki T, Kimura K, Arai G, et al. Study on dedicated drill bit design for carbon fiber reinforced polymer drilling with improved cutting mechanism. Compos Part A Appl Sci Manuf 2021;142:106259. https://doi.org/10.1016/j.compositesa.2020.106259.

[40] Xu J, An Q, Cai X, Chen M. Drilling machinability evaluation on new developed high-strength T800S/250F CFRP laminates. Int J Precis Eng Manuf 2013;14:1687–96. https://doi.org/10.1007/s12541-013-0252-2.

[41] Xu J, Li C, Dang J, El Mansori M, Ren F. A study on drilling high-strength CFRP laminates: frictional heat and cutting temperature. Mater (Basel, Switzerland) 2018;11:2366. https://doi.org/10.3390/ma11122366.

[42] Kaybal HB, Ünüvar A, Koyunbakan M, Avcı A. A novelty optimization approach for drilling of CFRP nanocomposite laminates. Int J Adv Manuf Technol 2019;100:2995–3012. https://doi.org/10.1007/s00170-018-2873-1.

[43] Geier N, Szalay T. Optimisation of process parameters for the orbital and conventional drilling of uni-directional carbon fibre-reinforced polymers (UD-CFRP). Measurement 2017;110:319–34. https://doi.org/10.1016/j.measurement.2017.07.007.

[44] Zheng B, Gao X, Li M, Deng T, Huang Z, Zhou H, et al. Formability and failure mechanisms of woven CF/PEEK composite sheet in solid-state thermoforming. Polymers (Basel) 2019:11. https://doi.org/10.3390/polym11060966.

[45] Xu J, Huang X, Chen M, Paulo DJ. Drilling characteristics of carbon/epoxy and carbon/polyimide composites. Mater Manuf Process 2020;00:1–9. https://doi.org/10.1080/10426914.2020.1784935.

[46] Geng D, Liu Y, Shao Z, Lu Z, Cai J, Li X, et al. Delamination formation, evaluation and suppression during drilling of composite laminates: A review. Compos Struct 2019;216:168–86. https://doi.org/10.1016/j.compstruct.2019.02.099.

[47] Babu J, Sunny T, Paul NA, Mohan KP, Philip J, Davim JP. Assessment of delamination in composite materials: A review. Proc Inst Mech Eng Part B J Eng Manuf 2015;230:1990–2003. https://doi.org/10.1177/0954405415619343.

[48] Higuchi R, Okabe T, Yoshimura A, Tay TE. Progressive failure under high-velocity impact on composite laminates: Experiment and phenomenological mesomodeling. Eng Fract Mech 2017;178:346–61. https://doi.org/10.1016/j.engfracmech.2017.03.019.

[49] Davim JP, Reis P. Study of delamination in drilling carbon fiber reinforced plastics (CFRP) using design experiments. Compos Struct 2003;59:481–7. https://doi.org/10.1016/S0263-8223(02)00257-X.

[50] Gaitonde VN, Karnik SR, Rubio JC, Correia AE, Abrão AM, Davim JP. Analysis of parametric influence on delamination in high-speed drilling of carbon fiber reinforced plastic composites. J Mater Process Technol 2008;203:431–8. https://doi.org/10.1016/j.jmatprotec.2007.10.050.

[51] Wang Q, Jia X. Optimization of cutting parameters for improving exit delamination, surface roughness, and production rate in drilling of CFRP composites. Int J Adv Manuf Technol 2021;117:3487–502. https://doi.org/10.1007/s00170-021-07918-2.

[52] Gaitonde VN, Karnik SR, Rubio JC, Correia AE, Abrão AM, Davim JP. A study aimed at minimizing delamination during drilling of CFRP composites. J Compos Mater 2011;45:2359–68. https://doi.org/10.1177/0021998311401087.

[53] Quiroga Cortés L, Caussé N, Dantras E, Lonjon A, Lacabanne C. Morphology and dynamical mechanical properties of poly ether ketone ketone (PEKK) with meta phenyl links. J Appl Polym Sci 2016:133. https://doi.org/10.1002/app.43396.

[54] Zhang W, Xu Y, Hui X, Zhang W. A multi-dwell temperature profile design for the cure of thick CFRP composite laminates. Int J Adv Manuf Technol 2021. https://doi.org/10.1007/s00170-021-07765-1.

[55] Matsuzaki R, Yokoyama R, Kobara T, Tachikawa T. Multi-objective curing optimization of carbon fiber composite materials using data assimilation and localized heating. Compos Part A Appl Sci Manuf 2019;119:61–72. https://doi.org/10.1016/j.compositesa.2019.01.021.

[56] Jung S, Choi W, Martins-Filho L, Madeira F. An implementation of self-organizing maps for airfoil design exploration via multi-objective optimization technique. J Aerosp Technol Manag 2016;8:193–202. https://doi.org/10.5028/jatm.v8i2.585.

[57] Molina-García J, García-Massó X, Estevan I, Queralt A. Built environment, psychosocial factors and active commuting to school in adolescents: clustering a self-organizing map analysis. Int J Environ Res Public Health 2019;16. https://doi.org/10.3390/ijerph16010083.

[58] Eneyew ED, Ramulu M. Experimental study of surface quality and damage when drilling unidirectional CFRP composites. J Mater Res Technol 2014;3:354–62. https://doi.org/10.1016/j.jmrt.2014.10.003.